

## Nuclear Magnetic Resonance Investigations of Intermetallic Compounds

Frank Haarmann, Marc Armbrüster, Daniel Grüner, Helge Rosner, and Yuri Grin

Nuclear magnetic resonance (NMR) experiments are a local probe of the electronic environment of nuclear spins. The signal of elements in non-magnetic compounds with nuclear spin  $I = 1/2$  is dominated by chemical shielding or Knight shift. For  $I > 1/2$  an additional contribution due to the coupling of the nuclear quadrupole moment with the electric field gradient has to be considered as a source of information [1]. Atomic disorder changes the local environments of the atoms and therefore, the electric field. This may result in resolvable NMR signals or in a broadening of the line shape. Two examples will be given: the first one is focused on atomic disorder in  $\text{Cu}_{1-x}\text{Al}_2$ , and the second example illustrates the influence of chemical bonding on NMR in the stannides  $M_4\text{Sn}_4$  of the alkali metals ( $M = \text{Na}, \text{K}, \text{Rb}, \text{Cs}$ ).

### Atomic disorder in $\text{Cu}_{1-x}\text{Al}_2$

$\text{Cu}_{1-x}\text{Al}_2$  crystallizes in its own structure type (Fig. 1) and details of the bonding situation as investigated by quantum mechanical methods, high-pressure X-ray diffraction, and Raman scattering have been described recently [2]. It is known [2, 3] that  $\text{Cu}_{1-x}\text{Al}_2$  shows a homogeneity range with  $0.028 \leq x \leq 0.044$  at  $T = 400^\circ\text{C}$ . Various contradicting models describing the local ordering of the atoms were discussed. An occupation of Cu sites by Al was favored in an NMR study [4] whereas occupation of Al positions by Cu atoms was deduced from a combined X-ray and mass density investigation [3].

Suitable isotopes for NMR experiments are  $^{63}\text{Cu}$  and  $^{65}\text{Cu}$  (nuclear spin  $I = 3/2$ ) as well as  $^{27}\text{Al}$  ( $I = 5/2$ ). Due to their nuclear spins these nuclei exhibit quadrupolar moments which give rise to line splitting. The  $^{63}\text{Cu}$  and  $^{65}\text{Cu}$  NMR signals of the main transition of  $\text{Cu}_{1-x}\text{Al}_2$  powder consist of several components (Fig. 2). Due to the non-cubic symmetry the compound is magnetically anisotropic. Thus, before performing NMR experiments, the crystallites were aligned in a magnetic field of approximately 12 T in order to increase the resolu-

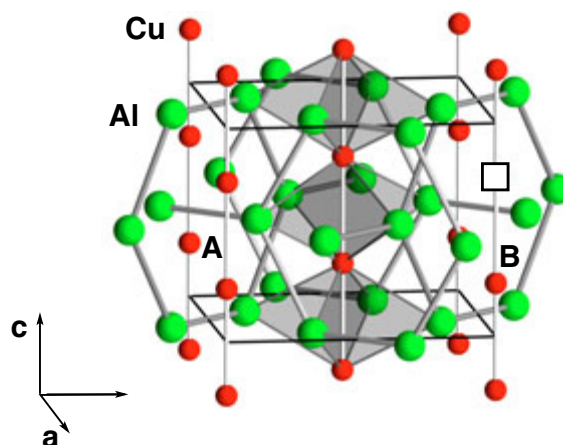


Fig. 1: Crystal structure and chemical bonding of  $\text{Cu}_{1-x}\text{Al}_2$  (two-center Al–Al bonds, grey sticks and three-center Cu–Al–Cu bonds, transparent triangles). A Cu vacancy is marked by a square. The Cu sites with different environments are marked by A and B, corresponding to the assignment of the NMR signals.

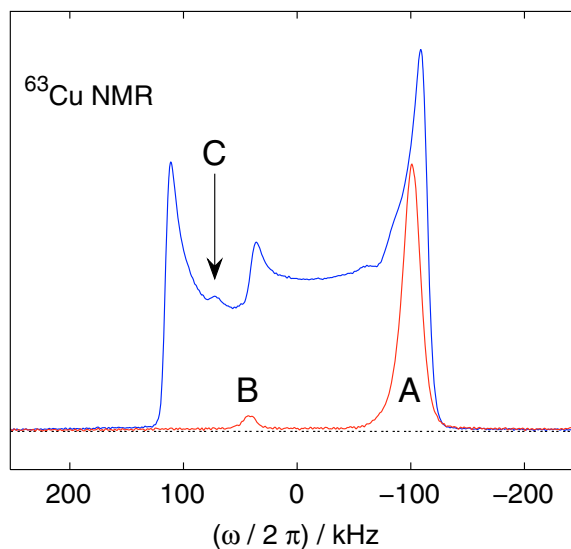


Fig. 2: NMR signal of the  $^{63}\text{Cu}$  central transition in a non-oriented (blue) and in a magnetically oriented sample of  $\text{Cu}_{1-x}\text{Al}_2$  (red line). The angle between orienting and external magnetic field is about  $45^\circ$ . The two signals are marked by A for the main and by B for the minority component.

tion of the NMR signals. Measurements of the oriented powder sample clearly indicate that the features in the line shape are due to two signals

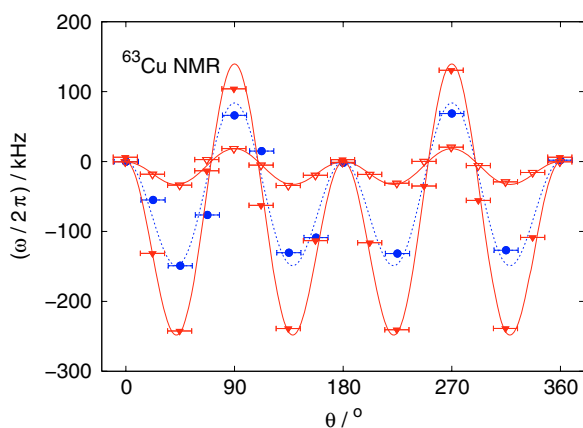


Fig. 3: Frequency shift of the  $^{63}\text{Cu}$  NMR signals of an oriented  $\text{Cu}_{1-x}\text{Al}_x$  sample in dependence of the angle between the magnetic fields applied for alignment and for measurement. Full symbols represent the main signal (A) and open symbols the minority signal (B). The lines show the calculated frequency shifts for  $B_0 = 11.74$  T (blue) and  $B_0 = 7.04$  T (red).

(Fig. 2). The ratio  $I_B / I_A$  of the signals A and B is about  $1 / 24$ .  $^{63}\text{Cu}$  NMR measurements of the sample with variation of the angle ( $\theta$ ) between the directions of the magnetic fields applied during the powder alignment and in the measurement show a characteristic frequency dependence of a second order quadrupole contribution to the main transition allowing the determination of the spectral parameter of both signals (Fig. 3). The quadrupolar frequency  $C_Q = (e^2 \cdot q \cdot Q) / h$  is calculated to yield 5.6 MHz and 15.4 MHz for signals B and A, respectively, assuming an axial symmetric electric field gradient ( $\eta = 0$ ). The quadrupolar frequencies are in good agreement with those extracted from the satellite positions providing a valuable prove of the assumption of  $\eta = 0$ .

Dipolar coupling of copper and aluminum nuclei were measured by means of Spin Echo Double Resonance experiments (SEDOR) [5]. The changes of the echo signal intensities with ( $S$ ) and without ( $S_0$ ) excitation of the potentially interacting nuclei are a probe of distance and orientation of the coupling nuclei with respect to the observed nuclei. We performed experiments for an orientation of  $\theta = 22^\circ$  and  $\theta = 45^\circ$ , investigating the interaction of  $^{65}\text{Cu} \leftrightarrow ^{63}\text{Cu}$  as well as  $^{65}\text{Cu} \leftrightarrow ^{27}\text{Al}$  of the signals A and B. Figure 4 shows the ratio of the echo amplitudes ( $S / S_0$ ). The  $^{65}\text{Cu}$  NMR echo amplitudes of signals A and B are almost identically reduced by coupling to the Al nuclei for both orientations of the sample. This indicates equivalent

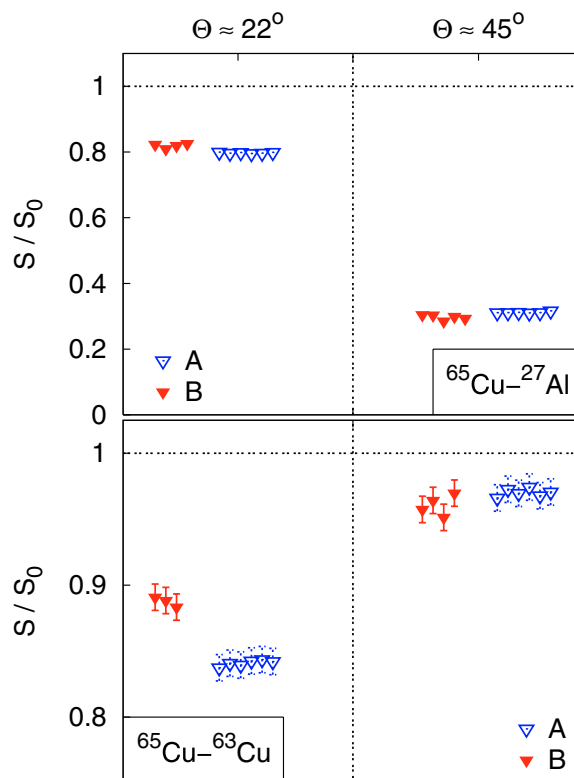


Fig. 4: Ratio  $S / S_0$  of the echo amplitudes of the  $^{65}\text{Cu}$  central transition measured by Spin Echo Double Resonance (SEDOR) for two orientations of the magnetically aligned sample ( $22^\circ$  and  $45^\circ$ ). Top:  $^{65}\text{Cu} \leftrightarrow ^{27}\text{Al}$  and bottom  $^{65}\text{Cu} \leftrightarrow ^{63}\text{Cu}$  experiments. Measurements of signal A are represented by blue and those of signal B by red symbols.

Al environments of both positions. The  $^{65}\text{Cu} \leftrightarrow ^{63}\text{Cu}$  coupling of signal A to A is larger than that of signal B to A for  $\theta = 22^\circ$ . This evidences the difference in the Cu environment of position A and B. For  $\theta = 45^\circ$ , the coupling differences are significantly reduced since the interaction is determined by  $D \propto (1/r^3) \cdot (1 - 3\cos^2\theta)$  resulting in a vanishing contribution of next neighbors for  $\theta = 54.75^\circ$ . The angular dependence clearly evidences that only the model of Cu vacancies is in agreement with both series of experiments ( $^{65}\text{Cu} \leftrightarrow ^{27}\text{Al}$  and  $^{65}\text{Cu} \leftrightarrow ^{63}\text{Cu}$ ). An occupation of the Cu sites by Al can obviously be ruled out on the basis of the  $^{65}\text{Cu} \leftrightarrow ^{27}\text{Al}$  measurements and an occupation of the Al sites by Cu by the  $^{65}\text{Cu} \leftrightarrow ^{63}\text{Cu}$  experiments.

In conclusion, the weak NMR signal (B) in  $\text{Cu}_{1-x}\text{Al}_x$  is caused by the reduction of the electric field gradient at the Cu sites neighboring a Cu vacancy. It is remarkable that, within experimental error, the shift of the signal is not influenced by the vacancies.

### Chemical bonding and NMR in $M_4Sn_4$ ( $M = \text{Na, K, Rb, Cs}$ )

The alkali metal monostannides  $M_4Sn_4$  ( $M = \text{Na, K, Rb, Cs}$ ) crystallize isostructurally to  $\text{Na}_4\text{Pb}_4$ . In this crystal structure, slightly distorted  $\text{Sn}_4^{4-}$  tetrahedra are built by four symmetry-equivalent, threefold-bonded Sn atoms. The anions are coordinated by two crystallographically independent alkali metal atoms: M1 located above the faces, and M2 above the edges of the tetrahedron. Four further M2 atoms give rise to a coordination number of 16 for the anion (Fig. 5). A systematic decrease of Sn-Sn bond lengths but no systematic change of bond angles was observed in single-crystal X-ray diffraction studies [6, 7]. The structural peculiarities of the alkali metal monostannides are investigated by combined application of  $^{119}\text{Sn}$  NMR spectroscopy, electronic band structure calculations,

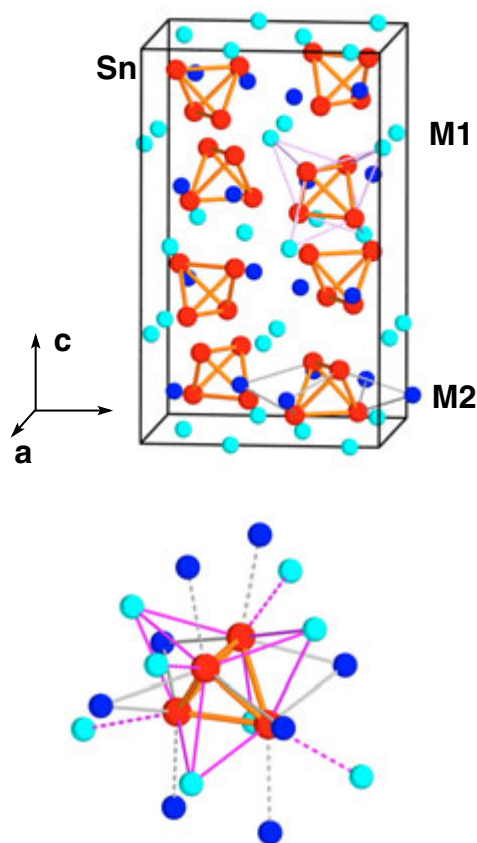


Fig. 5: Crystal structure of  $M_4Sn_4$  compounds with  $M = \text{Na, K, Rb, Cs}$  (top) and coordination of the  $\text{Sn}_4^{4-}$  tetrahedron (bottom). Tin atoms are represented in red and cations M1 and M2 by light blue and dark blue, respectively. The coordination of the  $\text{Sn}_4^{4-}$  tetrahedron by cations is marked by gray and pink bonds. The unit cell is marked by black lines.

and chemical bonding analysis by means of the electron localization function.

The  $^{119}\text{Sn}$  NMR signals of the alkali metal stannides  $M_4Sn_4$  are shifted towards low field (Fig. 6). Spectral parameters are obtained by least-squares fitting of the profiles assuming chemical shielding is the dominant interaction [8]. Whereas the anisotropy parameter does not show any tendency both the isotropic signal shift and the asymmetry parameter decrease with increasing size of cations. Since the distortion of the tetrahedron is virtually the same for all  $M_4Sn_4$  compounds, we analyze the chemical bonding and the electronic structure in order to rationalize the variations in NMR signal shift and shape.

An analysis of the electronic band structure and density of states indicates that the  $M_4Sn_4$  compounds are semiconducting, in agreement with experiment. In accordance with the presence of  $\text{Sn}_4^{4-}$  anions only Sn bonding bands are occupied. The bandwidth of the occupied bands decreases with increasing size of the cations and, therefore, increasing inter-molecular distance. However, a

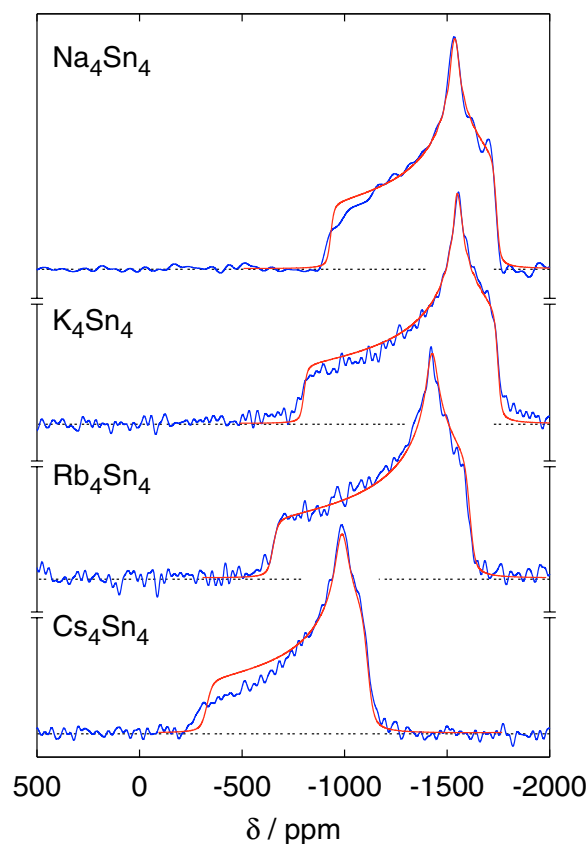


Fig. 6:  $^{119}\text{Sn}$  NMR signals of  $M_4Sn_4$  with  $M = \text{Na, K, Rb, Cs}$ . (blue lines) and simulated spectra (red lines). The signal shift is with respect to tetramethyl tin.

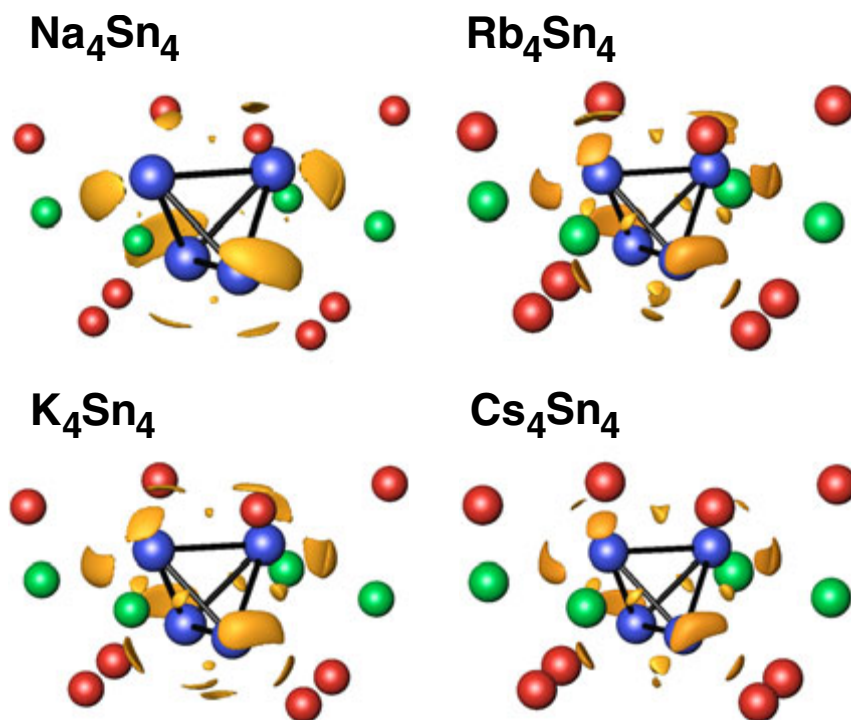


Fig. 7: Electron localization functions around  $\text{Sn}_4^{4-}$  anions in the crystal structures of  $M_4\text{Sn}_4$  with  $M = \text{Na}, \text{K}, \text{Rb}, \text{Cs}$ .

population analysis indicates that charge transfer is very small and does not change significantly within the  $M_4\text{Sn}_4$  series. Such a non-quantitative analysis of the electronic band structure is not suitable to explain the experimental trend in the change of the asymmetry parameter.

The  $^{119}\text{Sn}$  NMR signal shift within the  $M_4\text{Sn}_4$  series may be due to different charge transfer from alkali metal atoms to Sn. For that reason the charge transfer was analyzed using both *Bader's* Atoms-In-Molecules approach [9] and integration of charge in ELF basins. Although both methods clearly indicate charge transfer from alkali metal atoms to  $\text{Sn}_4^{4-}$  anions and yield comparable results regarding the number of electrons transferred, they do not indicate any tendency. Thus, the ELF topology was studied in more detail (Fig. 7). Besides nearly spherical attractors in the core regions of atoms, disynaptic attractors in the vicinity of Sn-Sn contacts indicate two-center bonds. Around an individual Sn atom, a group of monosynaptic attractors with respect to the Sn atoms is assigned to lone-pair like interactions. For an isolated  $\text{Sn}_4^{4-}$  molecule, only one such attractor located on the threefold axis is observed, but in the crystalline solid, the 'lone-pair' attractor splits in two ( $\text{Na}_4\text{Sn}_4$ ) or three ( $\text{K}_4\text{Sn}_4$ ,  $\text{Rb}_4\text{Sn}_4$ , and  $\text{Cs}_4\text{Sn}_4$ ) because of

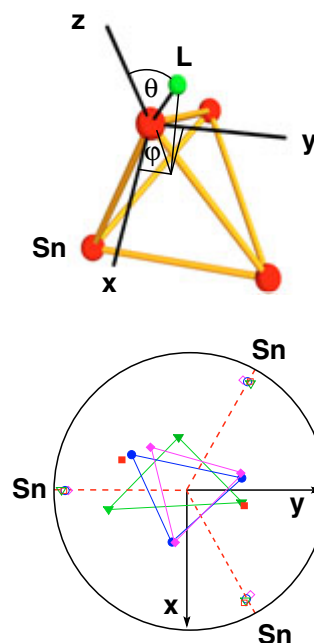


Fig. 8: (top) Coordinate system for the positions of the 'lone-pair' attractors in the alkali metal monostannides ( $\theta$  = polar angle,  $\varphi$  = azimuth) with respect to the anion. The  $z$  axis passes a Sn atom and the center of gravity. The  $x$  axis is in the mirror plane of the molecule. The position of an ELF maximum is marked by a circle. (bottom) Positions of the 'lone-pair' in projection along the  $z$  axis:  $\text{Na}_4\text{Sn}_4$  as red squares,  $\text{K}_4\text{Sn}_4$  as green triangles,  $\text{Rb}_4\text{Sn}_4$  as blue circles,  $\text{Cs}_4\text{Sn}_4$  as magenta diamonds.

the non-tetrahedral cationic environment of the atoms. The electron count of the respective basins decreases with increasing size of the cations whereas the electron count of the disynaptic attractors increases. This reflects the shortening of the intra-molecular Sn–Sn bonds with increasing size of the cations.

To compare the positions of the ‘lone-pair’ attractors in the  $M_4\text{Sn}_4$  compounds we introduce a polar coordinate system with the  $z$  axis long a line through the center of gravity and a Sn atom. The  $x$  axis is chosen within the mirror plane of the complex anion. The positions of the ELF maxima are schematically shown in Fig. 8. The two positions of the ELF maxima of  $\text{Na}_4\text{Sn}_4$  build a line with the  $z$  axis of the coordinate system approximately in the center. The triangle resulting from the three ELF maxima for  $M_4\text{Sn}_4$  with  $M = \text{K}, \text{Rb}, \text{Cs}$  becomes more regular with increasing radius of the cations. This indicates a gradual decrease of the anisotropy of charge distribution around a Sn atom from  $\text{Na}_4\text{Sn}_4$  to  $\text{Cs}_4\text{Sn}_4$  which correlates with the observed decrease of the  $^{119}\text{Sn}$  NMR asymmetry parameter.

## References

- [1] C. P. Slichter, Principles of Magnetic Resonance, Springer-Verlag, Berlin, Heidelberg, New York, third enlarged and updated edition (1990).
- [2] Yu. Grin, F. R. Wagner, M. Kohout, M. Armbrüster, A. Leithe-Jasper, U. Schwarz, U. Weding, H. G. von Schnering, J. Solid State Chem. submitted.
- [3] T. Gödecke, F. Sommer, Z. Metallkd. **87** (1996) 581.
- [4] T. J. Bastow, S. Celotto, Acta Materialia **51** (2003) 4621.
- [5] M. Emswiler, E. L. Hahn and D. Kaplan, Phys. Rev. **118** (1960) 414.
- [6] Yu. Grin, M. Baitinger, R. Kniep, H. G. von Schnering, Z. Kristallogr. NCS **214** (1999) 453.
- [7] M. Baitinger, Yu. Grin, R. Kniep, H. G. von Schnering, Z. Kristallogr. NCS **214** (1999) 457.
- [8] F. Haarmann, D. Grüner, H. Rosner, Yu. Grin, Z. Anorg. Allg. Chem. submitted.
- [9] R. F. W. Bader, Atoms in Molecules – A Quantum Theory, Clarendon Press, Oxford, 1995.